Published OnlineFirst February 24, 2015; DOI: 10.1158/2326-6066.CIR-14-0195

Research Article

Cancer Immunology Research

Individual Motile CD4$^+$ T Cells Can Participate in Efficient Multikilling through Conjugation to Multiple Tumor Cells

Ivan Liadi[1], Harjeet Singh[2], Gabrielle Romain[1], Nicolas Rey-Villamizar[3], Amine Merouane[3], Jay R T. Adolacion[1], Partow Kebriaei[4], Helen Huls[2], Peng Qiu[5], Badrinath Roysam[3], Laurence J.N. Cooper[2], and Navin Varadarajan[1]

Abstract

T cells genetically modified to express a CD19-specific chimeric antigen receptor (CAR) for the investigational treatment of B-cell malignancies comprise a heterogeneous population, and their ability to persist and participate in serial killing of tumor cells is a predictor of therapeutic success. We implemented Timelapse Imaging Microscopy in Nanowell Grids (TIMING) to provide direct evidence that CD4$^+$CAR$^+$ T cells (CAR4 cells) can engage in multikilling via simultaneous conjugation to multiple tumor cells. Comparisons of the CAR4 cells and CD8$^+$CAR$^+$ T cells (CAR8 cells) demonstrate that, although CAR4 cells can participate in killing and multikilling, they do so at slower rates, likely due to the lower granzyme B content. Significantly, in both sets of T cells, a minor subpopulation of individual T cells identified by their high motility demonstrated efficient killing of single tumor cells. A comparison of the multikiller and single-killer CAR$^+$ T cells revealed that the propensity and kinetics of T-cell apoptosis were modulated by the number of functional conjugations. T cells underwent rapid apoptosis, and at higher frequencies, when conjugated to single tumor cells in isolation, and this effect was more pronounced on CAR8 cells. Our results suggest that the ability of CAR$^+$ T cells to participate in multikilling should be evaluated in the context of their ability to resist activation-induced cell death. We anticipate that TIMING may be used to rapidly determine the potency of T-cell populations and may facilitate the design and manufacture of next-generation CAR$^+$ T cells with improved efficacy. *Cancer Immunol Res; 3(5); 473–82. ©2015 AACR.*

See related commentary by June, p. 470

Introduction

Chimeric antigen receptors (CAR) are hybrid molecules that typically combine the specificity and affinity of single-chain antibodies with selected intracellular signaling domains of the T-cell receptor complex (1–3; see glossary of abbreviations in Supplementary Information). When expressed on genetically modified T cells, CARs redirect specificity independently of human leukocyte antigen to recognize tumor-associated antigens (TAA). Second- and third-generation CARs include the endodomains for costimulatory molecules, and can thus directly endow the different signals needed for T-cell activation upon binding TAA (4). Initial data from clinical trials at multiple research centers reporting the adoptive transfer of T cells genetically modified to express a CD19-specific CAR for the treatment of B-cell malignancies are encouraging, with patients benefiting from complete remissions (5–7). These results have accelerated the clinical translation of T cells bearing CARs targeting TAAs other than CD19 for the treatment of hematologic malignancies as well as solid tumors (8–10). As a group, these clinical trials differ in the design and specificity of the CARs, the *ex vivo* approach used to manufacture the T cells, the *in vivo* regimen used to pretreat the recipient, the tumor burden and type, and the T-cell dosing scheme. Thus, drawing conclusions regarding the relative antitumor effects between the populations of bioengineered CAR$^+$ T cells is not readily feasible (1). One of the hallmarks of a therapeutically successful infusion is the presence of CAR$^+$ T cells that can persist to execute multiple tumor cells within the tumor microenvironment (11).

In spite of the recent success of adoptive immunotherapy, the mechanistic basis for the potency of a given T-cell product has not been well defined. The majority of adoptive studies have focused on infusing CD8$^+$ T-cell populations because of their ability to directly recognize and lyse tumor cells, thus mediating antitumor immunity (12). In the absence of CD4$^+$ T-cell help, however, some infused CD8$^+$ T cells can become functionally unresponsive and undergo apoptosis (13). Indeed, adoptive cell therapy protocols that incorporate CD4$^+$ T cells may mediate superior responses, and preclinical and clinical data have established the importance of CD4$^+$ T-cell help

[1]Department of Chemical and Biomolecular Engineering, University of Houston, Houston, Texas. [2]Division of Pediatrics, The University of Texas MD Anderson Cancer Center, Houston, Texas. [3]Department of Electrical Engineering, University of Houston, Houston, Texas. [4]Department of Stem Cell Transplantation and Cellular Therapy, The University of Texas MD Anderson Cancer Center, Houston, Texas. [5]Department of Biomedical Engineering, Georgia Institute of Technology and Emory University, Atlanta, Georgia.

Note: Supplementary data for this article are available at Cancer Immunology Research Online (http://cancerimmunolres.aacrjournals.org/).

I. Liadi and H. Singh contributed equally to this article.

Corresponding Author: Navin Varadarajan, Department of Chemical and Biomolecular Engineering, University of Houston, Houston, TX 77204. Phone: 713-743-1691; Fax: 713-743-4323; E-mail: nvaradar@central.uh.edu

doi: 10.1158/2326-6066.CIR-14-0195

Published OnlineFirst February 24, 2015; DOI: 10.1158/2326-6066.CIR-14-0195

during immunotherapy (14, 15). More recently, however, adoptive transfer of $CD4^+$ T-cell populations has shown that these cells can mediate regression of established melanoma, and that these cells can differentiate into cytolytic effectors (16–18). Despite these advances, direct comparisons of the potency and kinetics of interactions between donor-derived populations of $CD4^+$ T cells and tumor cells at single-cell resolution, and the comparison with $CD8^+$ T cells, are lacking.

Although two-photon microscopy studies are well suited for understanding the mechanistic basis of T-cell tumor cell interactions *in vivo*, direct observation of killing and motility is restricted to tens of events that may lead to sampling bias. In addition, these studies are limited in throughput and cannot be used to routinely determine the interactions between cellular infusions and tumor cells. *In vitro* dynamic imaging (19–24) systems are well-suited for studying the longitudinal interactions between cells at single-cell resolution, in a defined environment. Here, we have used Timelapse Imaging Microscopy in Nanowell Grids (TIMING) to analyze the longitudinal interactions between individual CD19-specific T cells (effectors, E) expressing a second-generation CAR with one or more $CD19^+$ tumor cells [target(s), T]. To the best of our knowledge, we demonstrate for the first time that $CD4^+CAR^+$ T cells (CAR4 cells) can directly engage in multikilling via simultaneous conjugation to multiple tumor cells. The major differences between CAR4 and $CD8^+$ CAR^+ T cells (CAR8 cells), at the single-cell, in mediating tumor-cell lysis *in vitro*, were the kinetics of killing, and this was attributed to the differences in their intracellular granzyme B content. Surprisingly, in both sets of T cells, a minor subpopulation of individual T cells identified by their high motility demonstrated efficient killing of single tumor cells. Comparison of the multikiller and single-killer CAR^+ T cells shows that the propensity and kinetics of T-cell apoptosis were modulated by the number of functional conjugations. Our results demonstrate that the ability of CAR^+ T cells to participate in multikilling should be evaluated in the context of their ability to resist activation-induced cell death (AICD).

Materials and Methods

Human subjects statement

All work outlined in this report was performed according to protocols approved by the Institutional Review Boards at the University of Houston and the University of Texas MD Anderson Cancer Center.

Cell lines and antibodies

All antibodies were purchased from BioLegend. The human pre-B cell line NALM-6 (ATCC), Daudi-β2m (ATCC), T-cell lymphoma EL-4 (ATCC), and modified $CD19^+$EL-4 cells were cultured as described previously (25, 26). The cell lines were routinely tested to ensure that they were free of *Mycoplasma* contamination and flow cytometry was used to confirm the expression of CD19.

Genetic modification and propagation of cells

Peripheral blood mononuclear cells (PBMC) from healthy volunteers were electroporated using Nucleofector II (Amaxa/Lonza) with DNA plasmids encoding for second-generation CAR (designated CD19RCD28) and SB11 transposase and cocultured with γ-irradiated K562 aAPC (clone 4) for 28 days along with cytokines (IL2 and IL21) in a 7-day stimulation cycle as described previously (25). For single-cell analysis, frozen CAR^+ T cells were revived and restimulated with irradiated K562 aAPC before using them in experiments.

Flow cytometry

Cells were stained for cell surface markers (CAR, CD4, CD8, and CD3), fixed and permeabilized (Cytofix/Cytoperm; BD Biosciences) for 20 minutes at 4°C. Cells were subsequently stained for intracellular granzyme B in perm/wash buffer at 4°C for 30 minutes, acquired on a FACS Calibur, and analyzed using FCS Express/FlowJo as previously described (25). Statistical analyses for determining granzyme B expression were performed within R.

Endpoint cytotoxicity assay

Nanowell array fabrication and the corresponding cytotoxicity assay to interrogate effector–target interaction at single-cell level were performed as described previously (21). Briefly, CAR^+ T cells labeled with 1 μmol/L of red fluorescent dye, PKH26 (Sigma) and target cells labeled with 1 μmol/L of green fluorescent dye PKH67 were coloaded onto nanowell arrays at a concentration of 10^6 cells/mL. Images were acquired on a Carl Zeiss Axio Observer fitted with a Hamamatsu EM-CCD camera using a 10× 0.3 NA objective. Automated image acquisition of the entire chip was performed at 0 and 6 hours and apoptosis was identified by staining with Annexin V conjugated to Alexa-647 (Life Technologies).

TIMING assays

Nanowell grids were fixed in position on a 60-mm petridish. The cells were labeled and loaded exactly as described for the endpoint assay and imaged on a Zeiss Axio Observer using a 20× 0.45 NA objective. Images were acquired for 12 to 16 hours at intervals of 7 to 10 minutes.

Statistical analysis

The test used to determine *P* values are listed in the legend of each figure.

Flow cytometry–based cytotoxicity assay

CAR4 cells (1×10^6 cells) were incubated with $CD19^+$ target cells (0.2×10^6 cells; Daudiβ_2m, NALM-6, and D19EL-4) at E:T ratio of 5:1 in the presence or absence of 5 mmol/L EGTA in 24-well plates in 5% CO_2 at 37°C for 6 hours. Following incubation cells were stained for CD3 (T cells) and CD19 (tumor targets), acquired on a FACS Calibur and analyzed using FCS Express version 3.00.007.

Supplementary Methods contain a description of the image segmentation and tracking algorithms.

Results

Production and phenotype of CAR^+ T cells

Genetically modified and propagated T cells were generated from the PBMCs of healthy volunteer donors derived using the Sleeping Beauty (SB) system (27), to enforce expression of a second-generation CD19-specific CAR (designated CD19RCD28) that activates T cells via a chimeric CD3 and CD28 endodomain (Fig. 1A). Subsequent to expansion, CAR^+ T cells from two separate donors contained predominantly $CD8^+$ T cells (Fig. 1B). The approach to producing the CAR^+ T cells mirrors our manufacture in compliance with current good manufacturing practice for human application (Supplementary Figs. S1 and S2).

Published OnlineFirst February 24, 2015; DOI: 10.1158/2326-6066.CIR-14-0195

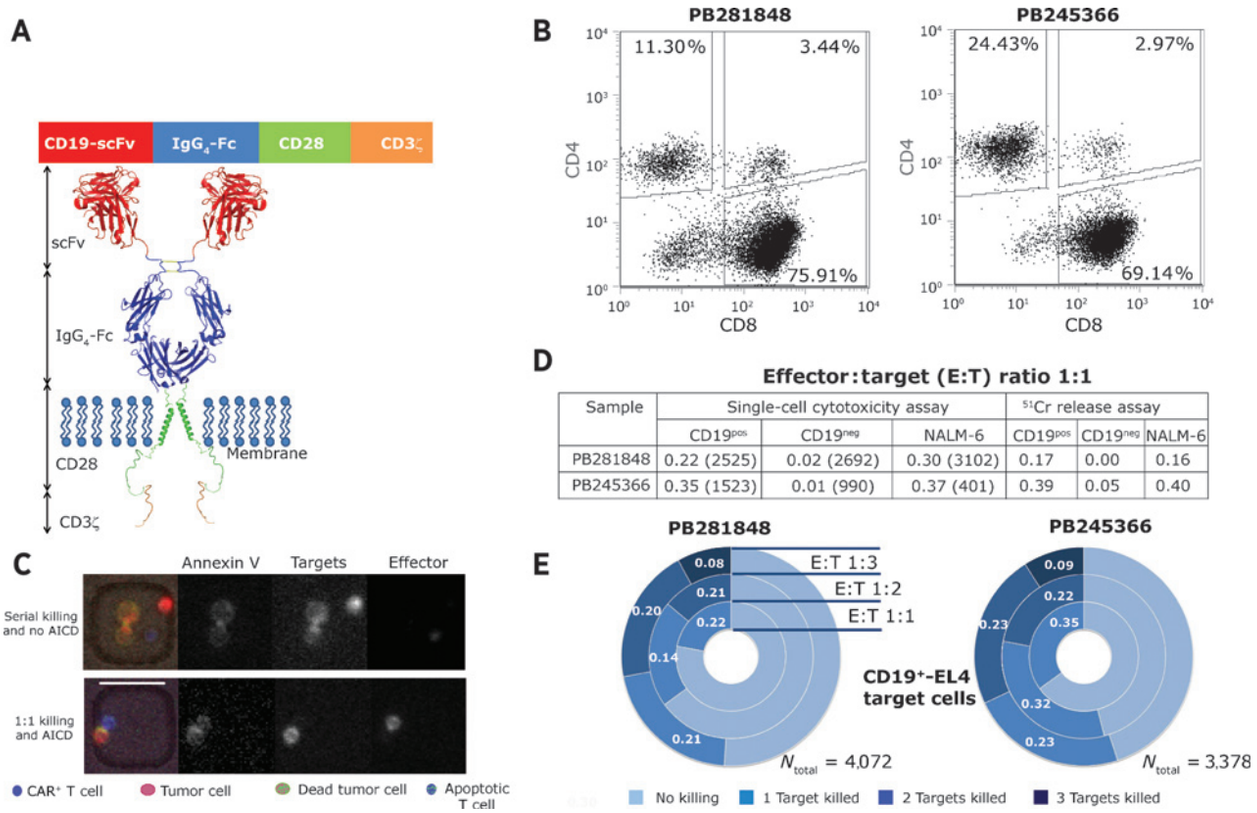

Sample	Single-cell cytotoxicity assay			^{51}Cr release assay		
	CD19^{pos}	CD19^{neg}	NALM-6	CD19^{pos}	CD19^{neg}	NALM-6
PB281848	0.22 (2525)	0.02 (2692)	0.30 (3102)	0.17	0.00	0.16
PB245366	0.35 (1523)	0.01 (990)	0.37 (401)	0.39	0.05	0.40

Figure 1.
High-throughput single-cell analysis of CAR$^+$ T-cell cytolytic functionality in nanowell grids. A, schematic of second-generation CD19-specific CAR (CD19RCD28) that signals through chimeric CD28/CD3-ζ. B, phenotypic characterization of the CAR$^+$ T cells from two separate donors. The total CD3$^+$CAR$^+$ population was gated to reveal the frequencies of CD4$^+$ and CD8$^+$ CAR$^+$ T-cell populations. C, representative composite micrographs illustrating the ability of single CAR$^+$ T cells to kill, and to undergo apoptosis, when incubated with tumor cells confined within nanowells; scale bar, 50 μm. D, comparison of the cytolytic responses measured by the single-cell assay and population-level ^{51}Cr release assay at an E:T ratio of 1:1. The numbers in parentheses for the single-cell assay indicate the total number of events observed. E, donut plots summarizing the frequency of killing outcomes of the interaction between CAR$^+$ T cells, derived from these two donors, and CD19$^+$ EL4 target cells. Representative micrographs illustrating each of these interactions are shown in Supplementary Fig. S5.

The cytotoxic potential, specificity, and multikilling ability of individual CAR$^+$ T cells

Donor-derived CAR$^+$ T-cell populations were evaluated for their ability to lyse CD19$^+$EL4 target cells, by coculture within nanowell grids (Fig. 1C and Supplementary Fig. S3). At an E:T of 1:1, averaged across both donors, 29% of single CAR$^+$ T cells induced apoptosis of (number of events, $N_{total} = 4{,}048$) CD19$^+$EL4 cells within 6 hours, whereas they induced apoptosis of just 1% ($N_{total} = 3{,}682$) of CD19$^-$EL4 cells in the same time frame. The >29-fold increase of lysis of CD19$^+$ versus CD19$^-$ targets confirms TAA-specific lysis (Fig. 1D, $P < 0.0001$, Fisher 2 × 2 test). In parallel, a conventional 4-hour ^{51}Chromium release assay (CRA) was performed at the same E:T ratio (1:1) and reported a similar overall magnitude of target cells killing (mean 14-fold increase of lysis of CD19$^+$ vs. CD19$^-$EL4 cells), albeit without single-cell resolution (Fig. 1D). The ability to redirect specificity to lyse human CD19$^+$ tumor cells was confirmed using the pre-B cell line NALM-6 (Supplementary Fig. S4). When averaged across both donors, within 6 hours of observation, individual CAR$^+$ T cells induced apoptosis in 34% ($N_{total} = 3{,}503$) of NALM-6 target cells at an E:T ratio of 1:1. Across all of the samples tested, single-cell assay demonstrated a linear correlation to the CRA (Fig. 1D, $r^2 = 0.84$, $P = 0.01$). The ability of individual T cells to eliminate more than one target cell was quantified by analyzing nanowells containing multiple targets (Supplementary Fig. S5). Averaged across both donors, at an E:T ratio of 1:2, within 6 hours, 21% ($N_{total} = 2{,}294$) of single CAR$^+$ T cells killed exactly one CD19$^+$ EL4 target-cell whereas 23% killed both targets (Fig. 1E). During this same timeframe, at an E:T ratio of 1:3, 22% ($N_{total} = 1{,}108$) of single CAR$^+$ T cells killed exactly one target, 22% killed exactly two targets, and 9% killed all three targets (Fig. 1E). Thus, within a defined observation window, the likelihood that an individual CAR$^+$ T cell killed more than one tumor cell improved as the number of targets within the nanowell increased, but this might simply reflect higher frequency of interactions at higher cell densities (Supplementary Fig. S6). These findings were also observed when substituting NALM-6 as target cells, albeit with diminished frequency of multikilling after 6 hours of coculture (Supplementary Fig. S7). In aggregate, these data demonstrate that the responses measured by the single-cell assay are consistent with the results of CRA, and that multikiller CAR$^+$ T cells (ability to lyse at least two targets) comprised 20% ($N_{total} = 3{,}402$) of the CAR$^+$ T-cell population.

Motile CD8$^+$ cytotoxic T cells are efficient killers with decreased potential for AICD

To gain an improved mechanistic understanding of the interaction between individual CAR$^+$ T cells and NALM-6 tumor cells, we

Published OnlineFirst February 24, 2015; DOI: 10.1158/2326-6066.CIR-14-0195

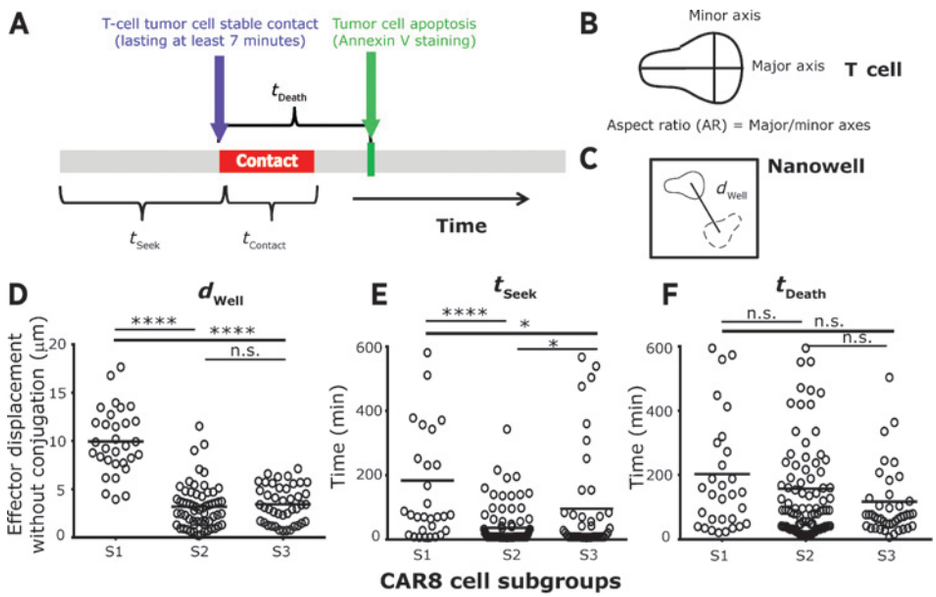

Figure 2.
CAR8 cells can be classified into different subgroups based on their motility and conjugation periods with NALM-6 tumor cell (E:T 1:1). A, schematic depicting the effector parameters used to describe their interaction with single NALM-6 tumor cells: red bar indicates periods of conjugation, blue arrow indicates time point at which conjugation was first observed, and green line indicates time to target death since first conjugation. B, the aspect ratio of polarization describes the ratio of major and minor axis fitted to an ellipse. C, d_{Well} represents the average displacement of the centroid of the effector cell between successive 7-minute time points. The mean: motility (D), time to first conjugation (E), and killing efficiency (F) of single CAR8 cells in each of three different subgroups. Each circle represents a single cell. *P* values for multiple comparisons were computed using parametric one-way ANOVA. *, $P < 0.05$; ****, $P < 0.0001$; n.s., not statistically significant.

developed and implemented TIMING (Supplementary Fig. S8). Six parameters describing T-cell intrinsic behavior motility (d_{Well}) and aspect ratio of polarization (AR), conjugation (contact lasting >7 minutes, t_{Seek} and $t_{Contact}$), and death (t_{Death} and t_{AICD}) were computed to define each interacting pair of effector and tumor cell (Fig. 2A–C). At an E:T of 1:1, 77% ($N_{total} = 268$) of single $CD8^+$ CAR^+ T cells (CAR8 cells) that made at least one conjugate were able to kill the engaged leukemia cell. To identify subgroups of T cells that exhibited different behavioral interactions with the tumor cells leading to subsequent killing, the time series data for each of three features, total duration of conjugation, d_{well}, and AR, were clustered hierarchically (Supplementary Fig. S9; ref. 28). Three T-cell subgroups were described that collectively accounted for 70% of the single-killer CAR8 cells: S1 [14% (7%–20%), range], low conjugation and high motility; S2 [49% (32%–66%)], high conjugation and low motility; and S3 [21% (19%–22%)], low conjugation and low motility (Supplementary Fig. S9). The high-motility subgroup, S1, comprised predominantly elongated T cells that had an initial "lag-phase" (t_{Seek} 184 ± 38 minutes, mean ± SEM), but formed stable conjugates ($t_{Contact}$ 98 ± 13 minutes) before target apoptosis (t_{Death} 204 ± 35 minutes; Fig. 2D–F and Supplementary Fig. S10). Predominantly, these T cells exhibited a decrease in motility and increased circularization (Supplementary Fig. S11) during tumor-cell conjugation, detached after tumor-cell death, resumed normal migratory function, and had only a low frequency of effector cells undergoing AICD (Supplementary Fig. S12, Movie M1). The representative cell in the dominant subgroup, S2, established conjugation quickly (t_{Seek} 36 ± 6 minutes) and displayed sustained conjugation ($t_{Contact}$ 145 ± 16 minutes) before killing (t_{Death} 158 ± 18 minutes; Fig. 2E–F). The majority of these T cells did not detach or resume migratory function after tumor-cell lysis, retained a predominantly circular morphology, and continued to remain conjugated >10 hours, even subsequent to the death of the conjugated tumor cell (Movie M2). Moreover, 88% of S2 effector cells underwent apoptosis within the first 10 hours of observation (Supplementary Fig. S12). Finally, T cells in the S3 subgroup were rapid killers ($t_{Contact}$ 84 ± 8 minutes and t_{Death} 118 ± 20 minutes) that arrested after conjugation, but failed to resume migration after tumor-cell detachment/killing (Fig. 2E–F and Movie M3). Although these S3 effectors detached from tumor cells after delivering the lethal hit, 53% then underwent apoptosis (Supplementary Fig. S12). Taken together, these results demonstrate that at an E:T ratio of 1:1, the dominant subgroup of cells, S2, identified by their lack of motility and early conjugation to tumor cells, underwent AICD. On the contrary, highly motile CAR8 cells, S1, detached efficiently and resumed exploration of the local microenvironment, indicating that the motility of CAR8 cells might help identify efficient killers with decreased propensity for AICD. The observation that the majority of the CAR8 cells (S2 subgroup) maintained extended contact even after the death of the tumor cell is consistent with investigations on HIV-specific CTLs (29).

CAR8 cell motility at increased tumor-cell densities facilitates multiplexed killing

The efficacy of CAR^+ T cells to eliminate tumor burden in excess of the number of effectors infused is due to their ability to persist and participate in serial killing (11). To facilitate identification of multikillers, we next profiled the interactions in nanowells containing a single CAR8 cell and 2 to 5 NALM-6 tumor cells (E:T 1:2–5). The frequency of CAR8 cells that were able to simultaneously conjugate to two or more tumor cells increased from 25% to 49% as the number of targets within the

Published OnlineFirst February 24, 2015; DOI: 10.1158/2326-6066.CIR-14-0195

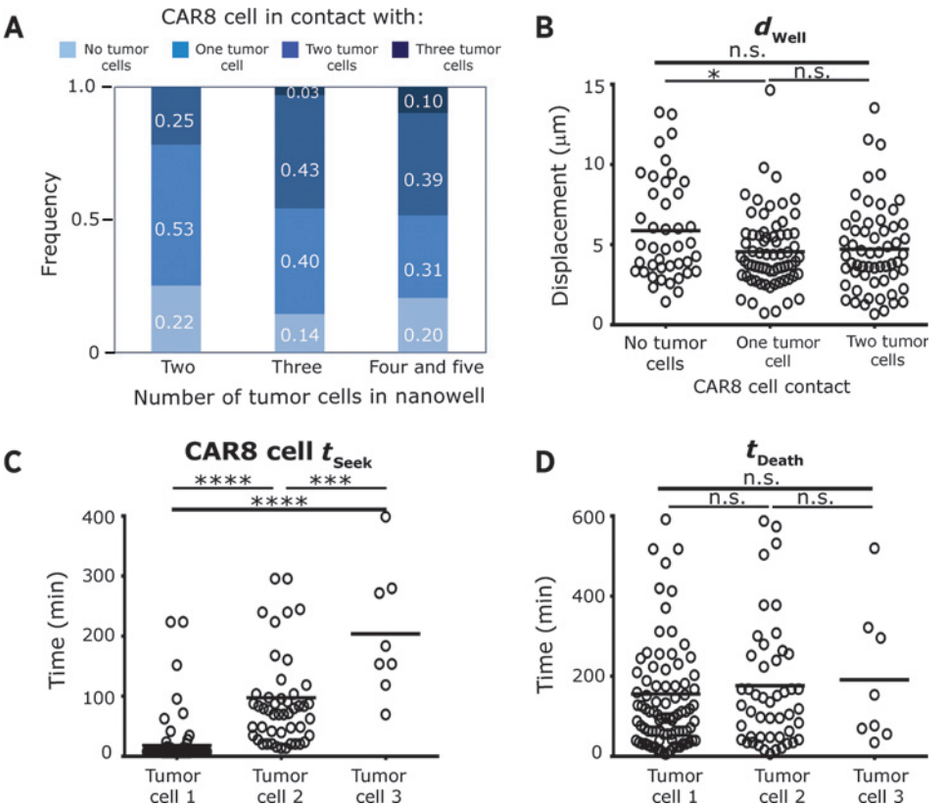

Figure 3.
Multikiller CAR8 cells engage in simultaneous conjugations leading to multiplexed killing (E:T 1:2-5). A, distribution of the number of simultaneous conjugations of individual CAR8 cells when incubated with increasing number of NALM-6 tumor cells. The mean: motility (B), time to first conjugation (C), and killing efficiency (D) of individual multikiller CAR8 cells. *P* values for multiple comparisons were computed using parametric one-way ANOVA. *, $P < 0.05$; ***, $P < 0.001$; ****, $P < 0.0001$; n.s., not statistically significant.

nanowell increased, indicating that multiplexed killing might be important (Fig. 3A and Movie M4). The frequency of simultaneous tumor conjugates that result in tumor cell deaths [46% (43%–50%)] was not very different from true serial killers that attach, kill, detach, and attach to a different tumor cell [49% (44%–53%)], suggesting that CAR8 cells are capable of eliciting either mode of killing, likely dependent on tumor cell density. Individual multikiller CAR8 cells ($N_{total} = 70$) demonstrated only a small decrease in motility when conjugated to one tumor cell, but showed no significant change in motility upon conjugation to multiple tumor cells [d_{Well}(unconjugated): 5.9 ± 0.5 μm vs. d_{Well} (single target): 4.6 ± 0.3 μm vs. d_{Well} (two targets): 4.7 ± 0.3 μm; Fig. 3B]. The only difference for multikillers when contacting the different tumor cells was in their time to establish conjugates (t_{Seek} $Target_1$: 18 ± 4 minutes vs. $Target_2$: 98 ± 13 minutes, Fig. 3C). Both duration of conjugation ($t_{Contact}Target_1$: 101 ± 9 minutes vs. $Target_2$: 113 ± 15 minutes) and killing efficiency ($t_{Death}Target_1$: 156 ± 17 minutes vs. $Target_2$: 177 ± 24 minutes) were no different (Fig. 3D and Supplementary Fig. S13). In addition to contact duration, the number of CAR8 cell–tumor cell conjugations that led to killing during encounter with the first tumor cells (61% both donors) was also not significantly different from the number of conjugations that resulted in target cell killing during encounter with the second tumor cell [74% (70%–79%)]. These TIMING data suggest that the efficiency to kill a second tumor cell is largely unaffected by the hit on a first target ($P > 0.99$). Furthermore, in comparison with single-killer CAR8 cells, multikiller CAR8 cells displayed greater motility when conjugated to the tumor cell despite the increased crowding because of higher tumor cell density (Supplementary Fig. S14).

Motility can identify a subgroup of CAR4 cells with enhanced cytotoxic efficiency

We have previously reported that the culture of CAR^+ T cells in the presence of IL2 and IL21 on aAPC can lead to outgrowth of CAR4 cells with cytotoxic potential (25). To facilitate comparisons with CAR8 cells, and to demonstrate that CAR4 can directly participate in killing and multikilling (Movie M5), the interaction of individual CAR4 cells from two donor–derived populations (Fig. 4A), with NALM-6 tumor cells was profiled using TIMING. At an E:T ratio of 1:1, 55% ($N_{total} = 549$) of single CAR4 cells that conjugated to an NALM-6 cell subsequently killed the tumor cell. As with the CAR8 cells, the interaction behavior of CAR4 cells with the NALM-6 cells could be classified into three subgroups, S1 to S3 (Supplementary Fig. S15). CAR4 cells in the enhanced motility subgroup, S1 (11% both donors), displayed significantly faster kinetics of tumor cell death (t_{Death} 157 ± 17 minutes) compared with the dominant S2 [34% (31%–36%)] subgroup (t_{Death} 318 ± 23 minutes, Fig. 4B–D). This increased kinetic efficiency was consistent with the decreased conjugation time required by the S1 subgroup of cells ($t_{Contact}$ 122 ± 11 minutes) in comparison with the S2 subgroup ($t_{Contact}$ 300 ± 21 minutes; Supplementary Fig. S16). These results suggest that, similar to CAR8 cells, the motility of the CAR4 cells may help identify the most efficient killers.

Both single-killer and multikiller CAR4 cells required longer conjugation and demonstrated delayed kinetics of killing in comparison with CAR8 cells

At the E:T ratio of 1:1, comparisons of the killing efficiency of CAR4 cells (t_{Death} 284 ± 11 minutes) and CAR8 cells (163 ± 12

Published OnlineFirst February 24, 2015; DOI: 10.1158/2326-6066.CIR-14-0195

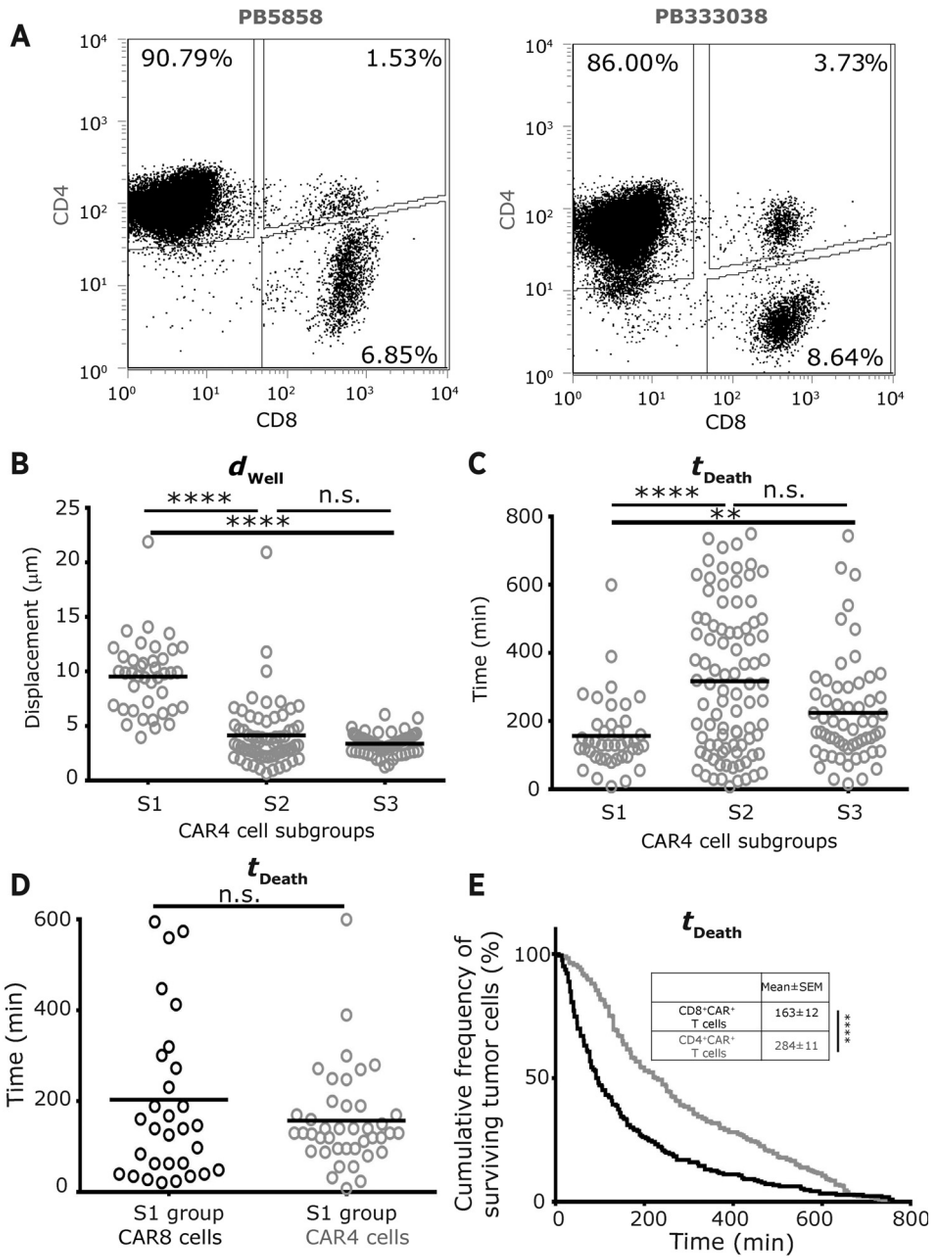

Figure 4.
Subpopulation of CAR4 cells, identified on the basis of their motility, can engage in efficient killing (E:T 1:1). A, phenotypic characterization of the CAR^+ T cells from two separate donors that comprise predominantly $CD4^+CAR^+$ T cells. The mean: motility (B) and killing efficiency (C) of single CAR4 cells in each of three different subgroups. D, comparison of the means of the killing efficiencies between single CAR8 and CAR4 cells within the S1 subgroups. Each circle represents a single cell in B, C, and D; CAR4 cells are represented by gray circles, and CAR8 cells are represented by black circles. E, comparative Kaplan–Meier estimators depicting the differences in killing efficiencies of the entire population of CAR4 cells and CAR8 cells. *P* values for multiple comparisons (B and C) were computed using a parametric one-way ANOVA, and dual comparisons (D and E) were computed using the unpaired two-tailed *t* test. *, $P < 0.05$; ****, $P < 0.0001$; n.s., not statistically significant.

minutes) demonstrated that individual CAR4 cells on average required 2 extra hours to induce tumor cell death (Fig. 4E). Consistent with the observation that the S2 subgroup is the dominant population of CAR^+ T cells, CAR4 cells in the S2 subgroup (t_{Death} 318 ± 23 minutes) demonstrated delayed kinetics of killing in comparison with CAR8 cells within the S2 subgroup (t_{Death} 158 ± 18 minutes; Supplementary Fig. S17). As mentioned above, because the motility of CAR4 cells could be used to identify the most efficient killers (Fig. 4C), comparisons of the kinetic efficiency of CAR4 cells in the S1 subgroup (t_{Death} 157 ± 17 minutes) with CAR8 cells in the S1 subgroup (t_{Death} 204 ± 34 minutes) demonstrated no significant differences. This finding further supports the notion that motility might be a useful parameter in identifying efficient cytolytic CAR^+ T cells. Comparisons of the single-cell behavioral interactions of multikiller CAR4 cells ($N_{total} = 78$) with the CAR8 cells demonstrated that most features were conserved across cells of both phenotypes. First, the unconjugated motility of CAR4 cells (d_{well} 6.9 ± 0.5 μm) was no different from that of CAR8 cells (d_{well} 5.9 ± 0.5 μm; Fig. 5A). Second, like CAR8 cells, CAR4 cells–demonstrated a matched decrease in motility (Fig. 5A) and increased circularization when conjugated to one or more tumor cells (Supplementary Fig. S18). Third, the preferred contact mode of the multikiller CAR4 cells was also simultaneous conjugations to multiple tumor cells (Supplementary Fig. S19 and Movie M5). Fourth, simultaneous conjugates that result in killing accounted for 61% (60%–63%) of multikilling events, indicating that this is an important mode of killing intrinsic to T cells and not just $CD8^+$ T cells. Fifth,

Published OnlineFirst February 24, 2015; DOI: 10.1158/2326-6066.CIR-14-0195

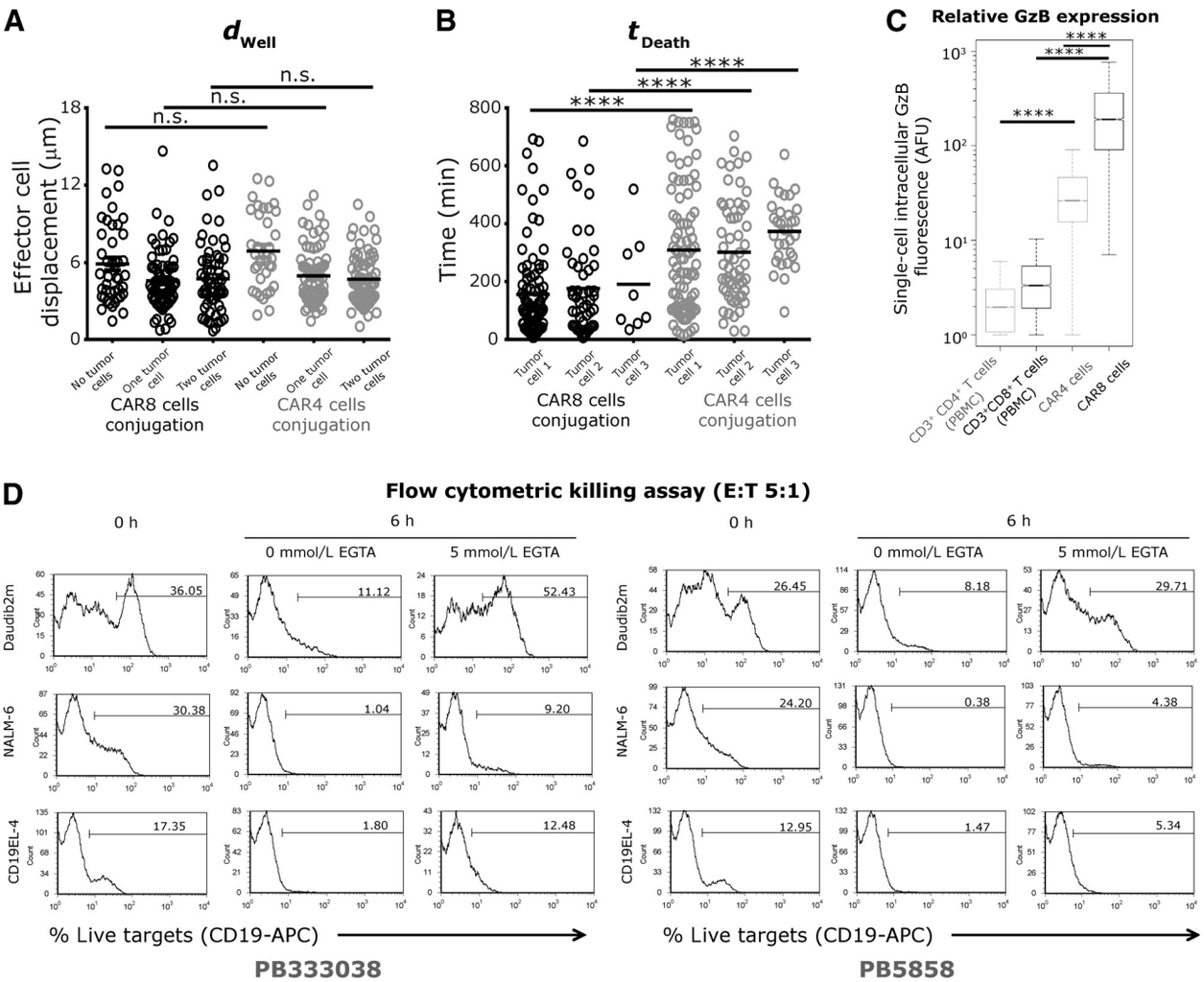

Figure 5.

Multikiller CAR4 cells demonstrated delayed kinetics of killing in comparison with CAR8 cells (E:T 1:2-5). Comparisons between the mean: motility (A) and killing efficiency (B) of single multikiller CAR8 cells and CAR4 cells. Each circle represents a single cell; CAR4 cells are represented by gray circles, and CAR8 cells are represented by black circles. C, box and whisker plots (extremities indicate 99% confidence intervals) displaying intracellular expression of granzyme B identified by immunofluorescent staining and flow cytometry. CAR4 cells (from donors PB5858 and PB333038) and CAR8 cells (from donors PB243566 and PB281848) were profiled using mAb against CD4/CD8/CAR and granzyme B. *P* values were computed using parametric one-way ANOVA for multiple comparisons or *t* tests for dual comparisons. D, flow cytometric killing assay (E:T = 5:1) of CAR4 cells incubated with three separate target cell lines (Daudi-β2m, NALM-6, and CD19$^+$EL4) in the absence or presence of 5 mmol/L EGTA blockade. ****, $P < 0.0001$; n.s., not statistically significant.

comparisons of t_{Death} for the different tumor cells killed by individual multikiller CAR4 cells demonstrated no differences (Fig. 5B). Finally, the number of CAR4 cell–tumor cell conjugations that lead to killing during the first tumor cell encounter [60% (58%–61%)] is not significantly different from the number of contacts that leads to killing when encountering the second tumor cell [60% (57%–63%)], suggesting that the killing efficiency is unchanged. Consistent with the observations at an E:T of 1:1, multikiller CAR4 cells required extended conjugation ($t_{Contact}$ 214 ± 18 minutes) and demonstrated slower kinetics before killing the first tumor cell (t_{Death} 310 ± 23 minutes) in comparison with CAR8 cells (Fig. 5B). In aggregate these results demonstrate that the major difference in CAR4 cells and CAR8 cells participating in either single killing or multikilling is the kinetics of tumor cell death.

Intracellular granzyme B content can explain differences in killing efficiency

To test the hypothesis that the varying efficiencies both between cells of the same population and in comparing CAR4 cells with CAR8 cells might be due to differences in expression of cytotoxic enzymes, we used intracellular staining at the single-cell level using flow cytometry to identify the expression of granzyme B within these cells. To establish baseline controls, the intracellular granzyme B content of CD3$^+$CD4$^+$ cells (2.36 ± 0.01) and CD3$^+$ CD8$^+$ cells (3.89 ± 0.04) in PBMC of two separate donors was determined (Fig. 5C). Consistent with our previous reports, both CAR4 cells (38.6 ± 0.2) and CAR8 cells (267 ± 2) showed significantly increased expression of granzyme B, in comparison with the controls (Fig. 5C). In agreement with the killing efficiency data (Fig. 5B), CAR4 cells expressed smaller amounts of granzyme

Published OnlineFirst February 24, 2015; DOI: 10.1158/2326-6066.CIR-14-0195

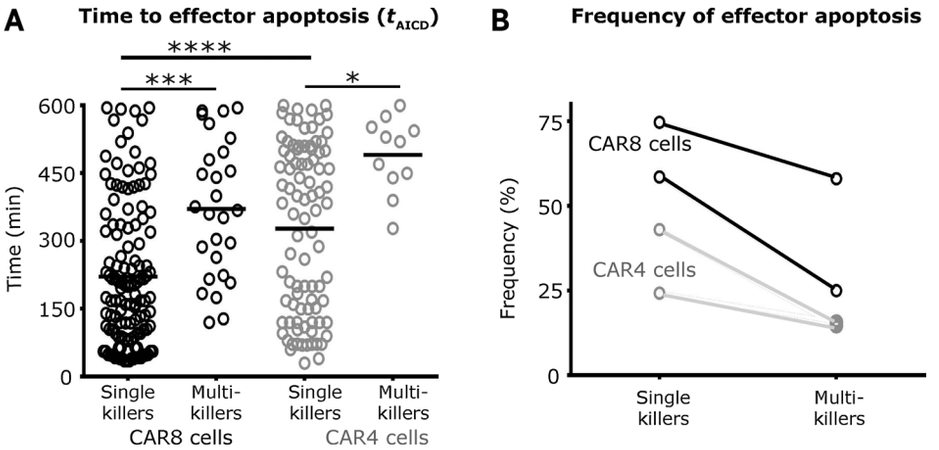

Figure 6.
Frequency and kinetics of killer cell apoptosis are dependent on functional conjugations with multiple NALM-6 tumor cells. A, comparisons of the mean kinetics of effector apoptosis of individual single killer CAR$^+$ T cells (E:T 1:1) with multikiller CAR$^+$ T cells (E:T 1:2-5). Each circle represents a single-cell; CAR4 cells are represented by gray circles, and CAR8 cells are represented by black circles. B, frequency of killer cell apoptosis as a function of tumor cell density. *, $P < 0.05$; ***, $P < 0.001$; ****, $P < 0.0001$; n.s., not statistically significant.

B in comparison with CAR8 cells, suggesting that the origin of the differing kinetic efficiencies of these cells might be the differences in granzyme B content (Fig. 5C).

To quantify the contribution of granzyme B secretion to tumor cell killing at the single-cell level, the ability of CAR4 cells to kill tumor cells in the presence of the calcium chelator EGTA was studied using flow cytometry (30). EGTA blocks cytotoxic granule exocytosis, and hence should eliminate granzyme B–mediated killing. Not surprisingly, CAR4 cells cocultured with tumor cells in the presence of 5 mmol/L EGTA demonstrated a substantial reduction in tumor cell killing across three different cell lines, Daudi-β2m, NALM-6, and CD19$^+$EL4 (Fig. 5D). The most striking reduction was seen with Daubi-β2m tumor cells, in which CAR4 cell–mediated killing was completely abolished (Fig. 5D).

CAR$^+$ T-cell fate is dependent on tumor-cell density

AICD is a mechanism by which T cells undergo programmed apoptosis in response to functional activation (31). The frequency and kinetics of individual cytolytic CAR$^+$ T cells to undergo AICD was monitored under the two conditions: at high and low tumor densities. CAR8 cells inducing apoptosis of single targets demonstrated significantly faster kinetics of AICD (t_{AICD} 221 ± 14 minutes) in comparison with the multikiller CAR8 cells from the same donors (t_{AICD} 371 ± 29 minutes, Fig. 6A). This trend of faster AICD kinetics at lower tumor cell density was also observed with CAR4 cells, albeit with delayed kinetics (Fig. 6A). Direct comparisons of the cells of different phenotypes at the same tumor cell density indicated that single-killer CAR8 cells underwent faster AICD (t_{AICD}, 221 ± 14 minutes) in comparison with CAR4 cells (t_{AICD} 328 ± 19 minutes; Fig. 6A). Consistent with the expectation that multikillers efficiently resist AICD, these T cells from three of four donors displayed low frequencies of cells undergoing AICD (13%–25%, Fig. 6B). However, multikiller T cells from the last donor displayed AICD at elevated frequencies (58%), underscoring that the efficiency of multikillers to execute multiple tumor cells must be evaluated in the context of their ability to resist AICD (Fig. 6B). We confirmed that the effector apoptosis that was observed required functional antigenic stimulation by coincubating CAR8 cells with CD19$^-$EL4 cells within nanowell grids and imaged them using TIMING. The frequency of apoptotic effectors under these conditions was only 4%, and this also confirmed that phototoxicity was negligible under the current imaging conditions.

Significantly, across all four donors, the frequencies of cytolytic CAR$^+$ T cells undergoing AICD were higher at an E:T of 1:1 in comparison with the multikiller CAR$^+$ T cells, and this effect was more exaggerated with CAR8 cells (Fig. 6B). These data may help account for the decrease in number and even disappearance of infused CAR$^+$ T cells when the CD19$^+$ tumor mass is reduced.

Discussion

We implemented a high-throughput single-cell assay (TIMING) to dynamically profile the functionality of CAR$^+$ T cells. Our analyses at the single-cell level demonstrate that, much like CAR8 cells, CAR4 cells can directly engage in tumor cell killing, albeit with altered kinetics. We further demonstrate that CAR4 cells can participate in multikilling via simultaneous conjugation to multiple tumor cells.

At low tumor cell densities (E:T 1:1), the majority of the single-killer CAR8 cells were significantly faster in killing tumor cells in comparison with individual CAR4 cells (Fig. 4E). By contrast, both single-killer CAR8 and CAR4 cells within the S1 subgroup, characterized by their high basal motility, displayed no significant differences in the kinetics of tumor cell killing. Furthermore, in contrast with the rest of the population, effector apoptosis was infrequent among CAR8 and CAR4 cells in the S1 subgroup. Collectively, these data suggested that the high basal motility of CAR$^+$ T cells (CAR4 or CAR8) might help identify efficient killers with decreased propensity for AICD.

When interacting with increased numbers of tumor cells (E:T ratios of 1:2 to 1:5), both individual CAR4 and CAR8 cells efficiently conjugated to multiple tumor cells, facilitating multiplexed killing. Comparisons among the different tumor cells by these individual multikiller CAR4/CAR8 cells demonstrated that they displayed an essentially unchanged efficiency ($t_{Contact}$) of killing of not only the first and second target, but also in comparison with (single-killer) CAR$^+$ T cells that were incubated with only one tumor cell (Supplementary Fig. S20). In comparing CAR4 cells with CAR8 cells, however, consistent with the observations at an E:T ratio of 1:1, CAR4 cells were significantly slower in tumor cell killing. Intracellular staining at the single-cell level indicated that the molecular origin of the differences in kinetic efficiency of the CAR4 and CAR8 cells could be attributed to their granzyme B content, and this was

Published OnlineFirst February 24, 2015; DOI: 10.1158/2326-6066.CIR-14-0195

further confirmed by blocking granule exocytosis using EGTA (Fig. 5).

For both CAR4 and CAR8 cells, single-killer effectors underwent apoptosis at higher frequencies and with faster kinetics in comparison with multikiller CAR$^+$ T cells (Figs. 1 and 4). These data indicate that activation for lysis through multiple targets as opposed to prolonged conjugation with a single target reduces the propensity for effector apoptosis. Although the mechanistic basis for the responsiveness of these T cells to antigen/target density is not known, it is conceivable that the continuous propagation of these cells on irradiated aAPC at defined ratios, allows for balanced activation while minimizing AICD (32). Collectively, these data could provide mechanistic insights into observations that infused CAR$^+$ T cells swell in number in response to addressing large numbers of CD19$^+$ tumor cells, but then decline in number as the tumor bioburden is lowered because of the multikilling by effector T cells (6, 33).

In aggregate, comparisons of the CAR4 cells and CAR8 cells demonstrate that, although CAR4 cells can participate in killing and multikilling, they do so at slower rates, likely due to the lower granzyme B content. This decreased kinetic efficiency, however, is likely a minor disadvantage and is counter balanced by their decreased propensity of these cells to undergo AICD in the absence of help from other cells, as profiled in our nanowell system. Indeed, recent preclinical and clinical data have suggested that complete eradication of established tumors can be accomplished by the adoptive transfer of T cells derived exclusively from CD4$^+$ T cells (16–18). Similarly, adoptive transfer of human T helper 17 (T_H17) cells has shown preclinical promise for the treatment of ovarian cancer (34, 35). Although we have focused on the heterogeneity among CAR$^+$ T cells, the results presented here are also likely influenced by the underlying heterogeneity in tumor cells. Although the expression of CD19 is uniform on the cells used as targets in our assays (Supplementary Fig. S4), it is feasible that there could be subpopulations of tumor cells that are resistant to CAR$^+$ T-cell–mediated killing.

Data from clinical trials have also shown a correlation between *in vivo* persistence of infused CAR$^+$ T cells and patient outcomes (36). Significantly, the findings of our short-term TIMING data (12-hour monitoring) that describe motility and ability to resist AICD as important attributes of functional T cells are consistent with persistence data obtained in mouse models infusing CD19-specific CAR$^+$ T cells that suggest that these same features are essential for tumor regression (37). Motility is likely a key parameter of the efficacy of T-cell therapies and has a significant role in tumor regression. It has been previously demonstrated that cancer cells from B-cell malignancies effectively dampen antitumor responses via disruption of actin-based basal T-cell motility *in vitro* (38–40). Second, the negative costimulatory molecules, PD-1 and CTLA4, have opposing effects on T-cell motility both *in vitro* and *in vivo* (41, 42). Finally, recent intravital microscopy data from melanoma models in mice have demonstrated that successful therapeutic anti-CTLA4 treatment correlates with greater T-cell motility (43).

The variation in the composition of CAR$^+$ T cells within a population of effector cells between donors across samples highlights the challenges in eliciting functional responsiveness in heterogeneous samples. As the field of adoptive immunotherapy takes on the challenge of targeting diseases that vary in burden, biodistribution, and antigen expression and density, it is important that *a priori* definitions of single-cell potency (proliferation, killing, cytokine secretion, etc.) be available. We suggest that identifying/quantifying specific biomarkers of efficacy, as described herein, may enable the manufacture of next-generation CAR$^+$ T cells.

Disclosure of Potential Conflicts of Interest

L.J.N. Cooper reports receiving commercial research grant from Immatics; has received speakers bureau honoraria from Miltenyi Biotec; has ownership interest (including patents) in Ziopharm, Intrexon, Sangamo Biosciences, and Targazyme; and is a consultant/advisory board member for Ferring Pharmaceuticals. No potential conflicts of interest were disclosed by the other authors.

Authors' Contributions

Conception and design: H. Singh, L.J.N. Cooper, N. Varadarajan
Development of methodology: I. Liadi, H. Singh, N. Rey-Villamizar, N. Varadarajan
Acquisition of data (provided animals, acquired and managed patients, provided facilities, etc.): I. Liadi, H. Singh, G. Romain, J.R.T. Adolacion
Analysis and interpretation of data (e.g., statistical analysis, biostatistics, computational analysis): I. Liadi, H. Singh, G. Romain, N. Rey-Villamizar, A. Merouane, J.R.T. Adolacion, P. Qiu, B. Roysam, L.J.N. Cooper, N. Varadarajan
Writing, review, and/or revision of the manuscript: I. Liadi, H. Singh, G. Romain, N. Rey-Villamizar, P. Kebriaei, P. Qiu, L.J.N. Cooper, N. Varadarajan
Administrative, technical, or material support (i.e., reporting or organizing data, constructing databases): I. Liadi, N. Rey-Villamizar, H. Huls, N. Varadarajan
Study supervision: L.J.N. Cooper, N. Varadarajan

Acknowledgments

The authors thank the flow-cytometry and fingerprinting cores at MDACC; Dr. June at the University of Pennsylvania for assistance with aAPC, Dr. Hackett at the University of Minnesota for the SB system; and Drs. McNamara, Mahendra, Kaul, and Ramesh for edits. J.R.T. Adolacion gratefully acknowledges the DOST-UP-ERDT Faculty Development Program.

Grant Support

This study was supported by funding from the NIH, including R01 (CA174385, CA124782, CA120956, CA141303, and CA163587); R33 (CA116127); Cancer Center Core Grant (CA16672); P01 (CA148600); SPORE (CA136411); and CPRIT (RP130570). Other support came from the MRA Stewart-Rahr Young Investigator Award; Welch Foundation (E1774); Adee Heebe, Ahuja family; Alex's Lemonade Stand Foundation; Burroughs Wellcome Fund; Gillson Longenbaugh Foundation; CLL Global Research Foundation; U.S. Department of Defense; National Foundation for Cancer Research; and Pediatric Cancer Research Foundation.

The costs of publication of this article were defrayed in part by the payment of page charges. This article must therefore be hereby marked *advertisement* in accordance with 18 U.S.C. Section 1734 solely to indicate this fact.

Received October 17, 2014; revised January 29, 2015; accepted February 16, 2015; published OnlineFirst February 24, 2015.

References

1. Kalos M, June CH. Adoptive T-cell transfer for cancer immunotherapy in the era of synthetic biology. Immunity 2013;39:49–60.
2. Sadelain M, Brentjens R, Riviere I. The basic principles of chimeric antigen receptor design. Cancer Discov 2013;3:388–98.

Published OnlineFirst February 24, 2015; DOI: 10.1158/2326-6066.CIR-14-0195

3. Dotti G, Gottschalk S, Savoldo B, Brenner MK. Design and development of therapies using chimeric antigen receptor-expressing T cells. Immunol Rev 2014;257:107–26.
4. Kochenderfer JN, Rosenberg SA. Treating B-cell cancer with T cells expressing anti-CD19 chimeric antigen receptors. Nat Rev Clin Oncol 2013;10: 267–76.
5. Brentjens RJ, Davila ML, Riviere I, Park J, Wang X, Cowell LG, et al. CD19-targeted T cells rapidly induce molecular remissions in adults with chemotherapy-refractory acute lymphoblastic leukemia. Sci Transl Med 2013;5:177ra138.
6. Grupp SA, Kalos M, Barrett D, Aplenc R, Porter DL, Rheingold SR, et al. Chimeric antigen receptor-modified T cells for acute lymphoid leukemia. N Engl J Med 2013;368:1509–18.
7. Jena B, Dotti G, Cooper LJ. Redirecting T-cell specificity by introducing a tumor-specific chimeric antigen receptor. Blood 2010;116:1035–44.
8. Spear P, Barber A, Sentman CL. Collaboration of chimeric antigen receptor (CAR)-expressing T cells and host T cells for optimal elimination of established ovarian tumors. Oncoimmunology 2013;2:e23564.
9. Morgan RA, Johnson LA, Davis JL, Zheng Z, Woolard KD, Reap EA, et al. Recognition of glioma stem cells by genetically modified T cells targeting EGFRvIII and development of adoptive cell therapy for glioma. Hum Gene Ther 2012;23:1043–53.
10. Louis CU, Savoldo B, Dotti G, Pule M, Yvon E, Myers GD, et al. Antitumor activity and long-term fate of chimeric antigen receptor-positive T cells in patients with neuroblastoma. Blood 2011;118:6050–6.
11. Kalos M, Levine BL, Porter DL, Katz S, Grupp SA, Bagg A, et al. T cells with chimeric antigen receptors have potent antitumor effects and can establish memory in patients with advanced leukemia. Sci Transl Med 2011;3: 95ra73.
12. Dudley ME, Yang JC, Sherry R, Hughes MS, Royal R, Kammula U, et al. Adoptive cell therapy for patients with metastatic melanoma: evaluation of intensive myeloablative chemoradiation preparative regimens. J Clin Oncol 2008;26:5233–9.
13. Janssen EM, Lemmens EE, Wolfe T, Christen U, von Herrath MG, Schoenberger SP. $CD4^+$ T cells are required for secondary expansion and memory in $CD8^+$ T lymphocytes. Nature 2003;421:852–6.
14. Antony PA, Piccirillo CA, Akpinarli A, Finkelstein SE, Speiss PJ, Surman DR, et al. $CD8^+$ T-cell immunity against a tumor/self-antigen is augmented by $CD4^+$ T helper cells and hindered by naturally occurring T regulatory cells. J Immunol 2005;174:2591–601.
15. Dudley ME, Wunderlich JR, Robbins PF, Yang JC, Hwu P, Schwartzentruber DJ, et al. Cancer regression and autoimmunity in patients after clonal repopulation with antitumor lymphocytes. Science 2002;298:850–4.
16. Hunder NN, Wallen H, Cao J, Hendricks DW, Reilly JZ, Rodmyre R, et al. Treatment of metastatic melanoma with autologous $CD4^+$ T cells against NY-ESO-1. N Engl J Med 2008;358:2698–703.
17. Quezada SA, Simpson TR, Peggs KS, Merghoub T, Vider J, Fan X, et al. Tumor-reactive CD4(+) T cells develop cytotoxic activity and eradicate large established melanoma after transfer into lymphopenic hosts. J Exp Med 2010;207:637–50.
18. Xie Y, Akpinarli A, Maris C, Hipkiss EL, Lane M, Kwon EK, et al. Naive tumor-specific CD4(+) T cells differentiated *in vivo* eradicate established melanoma. J Exp Med 2010;207:651–67.
19. Roach KL, King KR, Uygun BE, Kohane IS, Yarmush ML, Toner M. High-throughput single-cell bioinformatics. Biotechnol Prog 2009;25:1772–9.
20. Deutsch M, Deutsch A, Shirihai O, Hurevich I, Afrimzon E, Shafran Y, et al. A novel miniature cell retainer for correlative high-content analysis of individual untethered non-adherent cells. Lab Chip 2006;6:995–1000.
21. Liadi I, Roszik J, Romain G, Cooper LJ, Varadarajan N. Quantitative high-throughput single-cell cytotoxicity assay for T cells. J Vis Exp, 2013;72: e50058.
22. Yamanaka YJ, Berger CT, Sips M, Cheney PC, Alter G, Love JC. Single-cell analysis of the dynamics and functional outcomes of interactions between human natural killer cells and target cells. Integr Biol 2012;4:1175–84.
23. Vanherberghen B, Olofsson PE, Forslund E, Sternberg-Simon M, Khorshidi MA, Pacouret S, et al. Classification of human natural killer cells based on migration behavior and cytotoxic response. Blood 2013;121:1326–34.
24. Romain G, Senyukov V, Rey-Villamizar N, Merouane A, Kelton W, Liadi I, et al. Antibody Fc-engineering improves frequency and promotes kinetic boosting of serial killing mediated by NK cells. Blood 2014; 124:3241–9.
25. Singh H, Figliola MJ, Dawson MJ, Huls H, Olivares S, Switzer K, et al. Reprogramming CD19-specific T cells with IL-21 signaling can improve adoptive immunotherapy of B-lineage malignancies. Cancer Res 2011;71: 3516–27.
26. Singh H, Figliola MJ, Dawson MJ, Olivares S, Zhang L, Yang G, et al. Manufacture of clinical-grade CD19-specific T cells stably expressing chimeric antigen receptor using Sleeping Beauty system and artificial antigen presenting cells. PLoS ONE 2013;8:e64138.
27. Izsvak Z, Ivics Z. Sleeping beauty transposition: biology and applications for molecular therapy. Mol Ther 2004;9:147–56.
28. Lex A, Streit M, Schutz HJ, Partl C, Schmalstieg D, Park PJ, et al. StratomeX: visual analysis of large-scale heterogeneous genomics data for cancer subtype characterization. Comput Graph Forum 2012;31:1175–84.
29. Foley MH, Forcier T, McAndrew E, Gonzalez M, Chen H, Juelg B, et al. High avidity $CD8^+$ T cells efficiently eliminate motile HIV-infected targets and execute a locally focused program of anti-viral function. PLoS ONE 2014;9: e87873.
30. Henkart PA, Millard PJ, Reynolds CW, Henkart MP. Cytolytic activity of purified cytoplasmic granules from cytotoxic rat large granular lymphocyte tumors. J Exp Med 1984;160:75–93.
31. Krammer PH, Arnold R, Lavrik IN. Life and death in peripheral T cells. Nat Rev Immunol 2007;7:532–42.
32. Romer PS, Berr S, Avota E, Na SY, Battaglia M, ten Berge I, et al. Preculture of PBMCs at high cell density increases sensitivity of T-cell responses, revealing cytokine release by CD28 superagonist TGN1412. Blood 2011;118: 6772–82.
33. Kochenderfer JN, Dudley ME, Feldman SA, Wilson WH, Spaner DE, Maric I, et al. B-cell depletion and remissions of malignancy along with cytokine-associated toxicity in a clinical trial of anti-CD19 chimeric-antigen-receptor-transduced T cells. Blood 2012;119:2709–20.
34. Kryczek I, Zhao E, Liu Y, Wang Y, Vatan L, Szeliga W, et al. Human TH17 cells are long-lived effector memory cells. Sci Transl Med 2011;3:104ra100.
35. Kryczek I, Banerjee M, Cheng P, Vatan L, Szeliga W, Wei S, et al. Phenotype, distribution, generation, and functional and clinical relevance of Th17 cells in the human tumor environments. Blood 2009;114:1141–9.
36. Zhou J, Dudley ME, Rosenberg SA, Robbins PF. Persistence of multiple tumor-specific T-cell clones is associated with complete tumor regression in a melanoma patient receiving adoptive cell transfer therapy. J Immunother 2005;28:53–62.
37. Xu Y, Zhang M, Ramos CA, Durett A, Liu E, Dakhova O , et al. Closely related T-memory stem cells correlate with *in vivo* expansion of CAR. CD19-T cells and are preserved by IL-7 and IL-15. Blood 2014;123:3750–9.
38. Kiaii S, Clear AJ, Ramsay AG, Davies D, Sangaralingam A, Lee A, et al. Follicular lymphoma cells induce changes in T-cell gene expression and function: potential impact on survival and risk of transformation. J Clin Oncol 2013;31:2654–61.
39. Gorgun G, Holderried TA, Zahrieh D, Neuberg D, Gribben JG. Chronic lymphocytic leukemia cells induce changes in gene expression of CD4 and CD8 T cells. J Clin Invest 2005;115:1797–805.
40. Ramsay AG, Clear AJ, Kelly G, Fatah R, Matthews J, Macdougall F, et al. Follicular lymphoma cells induce T-cell immunological synapse dysfunction that can be repaired with lenalidomide: implications for the tumor microenvironment and immunotherapy. Blood 2009;114: 4713–20.
41. Zinselmeyer BH, Heydari S, Sacristán C, Nayak D, Cammer M, Herz J, et al. PD-1 promotes immune exhaustion by inducing antiviral T-cell motility paralysis. J Exp Med 2013;210:757–74.
42. Schneider H, Downey J, Smith A, Zinselmeyer BH, Rush C, Brewer JM, et al. Reversal of the TCR stop signal by CTLA-4. Science 2006;313:1972–5.
43. Pentcheva-Hoang T, Simpson TR, Montalvo-Ortiz W, Allison JP. Cytotoxic T lymphocyte antigen-4 blockade enhances antitumor immunity by stimulating melanoma-specific T-cell motility. Cancer Immunol Res 2014;2: 970–80.

Published OnlineFirst February 24, 2015; DOI: 10.1158/2326-6066.CIR-14-0195

Cancer Immunology Research

Individual Motile CD4$^+$ T Cells Can Participate in Efficient Multikilling through Conjugation to Multiple Tumor Cells

Ivan Liadi, Harjeet Singh, Gabrielle Romain, et al.

Cancer Immunol Res 2015;3:473-482. Published OnlineFirst February 24, 2015.